molecular pharmaceutics

articles

Site-Specifically Biotinylated $VEGF_{121}$ for Near-Infrared Fluorescence Imaging of Tumor Angiogenesis

Hui Wang, Kai Chen, Gang Niu, and Xiaoyuan Chen*

Molecular Imaging Program at Stanford, Department of Radiology & Bio-X Program, Stanford University School of Medicine, Stanford, California 94305-5484

Received September 30, 2008; Revised Manuscript Received November 17, 2008; Accepted November 26, 2008

Abstract: The vascular endothelial growth factor (VEGF)/VEGF receptor (VEGFR) pathway is considered to be one of the most important regulators of angiogenesis and a key target in anticancer treatment. Imaging VEGFR expression can serve as a new paradigm for assessing the efficacy of antiangiogenic cancer therapy, improving cancer management, and elucidating the role and modulation of VEGF/VEGFR signaling during cancer development and intervention. In this study we developed an Avi-tagged $VEGF_{121}$ protein, which is site-specifically biotinylated in the presence of bacterial BirA biotin ligase. BirA biotinylated $VEGF_{121}$-Avi ($VEGF_{121}$-Avib) forms a stable complex with streptavidin-IRDye800 (SA800) that retains high affinity for VEGFR *in vitro* and allows receptor specific targeting *in vivo* in a 67NR murine xenograft model. In contrast, chemical coupling of IRDye800 abrogated the VEGFR binding ability of the modified protein both *in vitro* and *in vivo*. The $VEGF_{121}$-Avib/SA800 complex (VEGF-Avib/SA800) may be used for quantitative and repetitive near-infrared fluorescence imaging of VEGFR expression and translated into clinic for evaluating cancer and other angiogenesis related diseases.

Keywords: Vascular endothelial growth factor (VEGF); Avi-tag; site-specific biotinylation; near-infrared fluorescence imaging; angiogenesis

Introduction

The vascular endothelial growth factor (VEGF)/VEGF receptor (VEGFR) pathway is considered to be one of the most important regulators of angiogenesis and a key target in anticancer treatment.[1,2] Increased expression of VEGF by tumor cells and VEGFR-2/KDR and VEGFR-1/Flt by the tumor-associated vasculature is a hallmark of a solid tumors, which correlates with tumor growth rate, microvessel density/proliferation, tumor metastatic potential, and poorer patient prognosis in a variety malignancies.[3] Targeted therapies that selectively inhibit the VEGF/VEGFR pathway have found widespread applicability.[4−8] VEGF/VEGFR-targeted molecular imaging can serve as a new paradigm for assessing the efficacy of antiangiogenic cancer therapy, improving cancer management, and elucidating the role and modulation of VEGF/VEGFR signaling during cancer development and intervention.

* Correspondence should be sent to this author. Mailing address: The Molecular Imaging Program at Stanford (MIPS), Department of Radiology and Bio-X Program, Stanford University School of Medicine, 1201 Welch Rd, P095, Stanford, CA 94305-5484. E-mail: shawchen@stanford.edu. Tel: 650-725-0950. Fax: 650-736-7925.

(1) Ferrara, N. VEGF and the quest for tumour angiogenesis factors. *Nat. Rev. Cancer* **2002**, *2*, 795–803.

(2) Roodhart, J. M.; Langenberg, M. H.; Witteveen, E.; Voest, E. E. The molecular basis of class side effects due to treatment with inhibitors of the VEGF/VEGFR pathway. *Curr. Clin. Pharmacol.* **2008**, *3*, 132–43.

(3) Underiner, T. L.; Ruggeri, B.; Gingrich, D. E. Development of vascular endothelial growth factor receptor (VEGFR) kinase inhibitors as anti-angiogenic agents in cancer therapy. *Curr. Med. Chem.* **2004**, *11*, 731–45.

(4) Sun, J.; Wang, D. A.; Jain, R. K.; Carie, A.; Paquette, S.; Ennis, E.; Blaskovich, M. A.; Baldini, L.; Coppola, D.; Hamilton, A. D.; Sebti, S. M. Inhibiting angiogenesis and tumorigenesis by a synthetic molecule that blocks binding of both VEGF and PDGF to their receptors. *Oncogene* **2005**, *24*, 4701–9.

(5) Watanabe, H.; Mamelak, A. J.; Wang, B.; Howell, B. G.; Freed, I.; Esche, C.; Nakayama, M.; Nagasaki, G.; Hicklin, D. J.; Kerbel, R. S.; Sauder, D. N. Anti-vascular endothelial growth factor receptor-2 (Flk-1/KDR) antibody suppresses contact hypersensitivity. *Exp. Dermatol.* **2004**, *13*, 671–81.

10.1021/mp800185h CCC: $40.75
Published on Web 12/19/2008

$VEGF_{121}$ protein has high binding affinity for VEGFR-2 and serves as an excellent candidate for imaging VEGFRs. Several studies have been reported on the use of appropriately labeled VEGF proteins for positron emission tomography (PET),[9−11] single-photon emission computed tomography (SPECT),[12−14] ultrasound,[8,15,16] and optical imaging.[17] However, most of the reported VEGF-based imaging agents are unsuitable for clinical translation because of the unacceptably high major organ, such as liver and kidney, uptake,[18] or uncertain binding activity of the protein, owing to damages caused by random radiolabeling or bioconjugation.[12,19−21] Therefore, site-specific modification of VEGF without changing the conformation of the protein and compromising its functional activity is required.

Avi-tag is a 14-amino acid peptide which contains a central lysine residue that can be biotinylated at the epsilon amine group by the bacterial BirA biotin ligase. Coexpression of BirA and Avi-fused protein in cells allows for facile detection and recovery of interested protein by existing avidin/streptavidin technology.[22] Here, we report for the first time the development of Avi-tagged $VEGF_{121}$ protein for imaging VEGFR expression in living objects. We fused an Avi-tag to the C-terminus of $VEGF_{121}$ to allow site-specific biotinylation with defined one-to-one stoichiometry without disruption of $VEGF_{121}$ function. The biotinylated $VEGF_{121}$-Avi (VEGF-Avib) was able to form a stable complex with streptavidin-IRDy800 (SA800), and the resulting VEGF-Avib/SA800 (Scheme 1) was used as a near-infrared fluorescence (NIRF) probe to image VEGFR expression in a 67NR murine breast cancer xenograft model. This probe could potentially be used for quantifiable and repetitive imaging of VEGFR expression during and after antiangiogenic treatment.

(6) Prewett, M.; Huber, J.; Li, Y.; Santiago, A.; O'Connor, W.; King, K.; Overholser, J.; Hooper, A.; Pytowski, B.; Witte, L.; Bohlen, P.; Hicklin, D. J. Antivascular endothelial growth factor receptor (fetal liver kinase 1) monoclonal antibody inhibits tumor angiogenesis and growth of several mouse and human tumors. *Cancer Res.* **1999**, *59*, 5209–18.

(7) Wedge, S. R.; Ogilvie, D. J.; Dukes, M.; Kendrew, J.; Curwen, J. O.; Hennequin, L. F.; Thomas, A. P.; Stokes, E. S.; Curry, B.; Richmond, G. H.; Wadsworth, P. F. ZD4190: an orally active inhibitor of vascular endothelial growth factor signaling with broad-spectrum antitumor efficacy. *Cancer Res.* **2000**, *60*, 970–5.

(8) Wood, J. M.; Bold, G.; Buchdunger, E.; Cozens, R.; Ferrari, S.; Frei, J.; Hofmann, F.; Mestan, J.; Mett, H.; O'Reilly, T.; Persohn, E.; Rosel, J.; Schnell, C.; Stover, D.; Theuer, A.; Towbin, H.; Wenger, F.; Woods-Cook, K.; Menrad, A.; Siemeister, G.; Schirner, M.; Thierauch, K. H.; Schneider, M. R.; Drevs, J.; Martiny-Baron, G.; Totzke, F. PTK787/ZK 222584, a novel and potent inhibitor of vascular endothelial growth factor receptor tyrosine kinases, impairs vascular endothelial growth factor-induced responses and tumor growth after oral administration. *Cancer Res.* **2000**, *60*, 2178–89.

(9) Nagengast, W. B.; de Vries, E. G.; Hospers, G. A.; Mulder, N. H.; de Jong, J. R.; Hollema, H.; Brouwers, A. H.; van Dongen, G. A.; Perk, L. R.; Lub-de Hooge, M. N. In vivo VEGF imaging with radiolabeled bevacizumab in a human ovarian tumor xenograft. *J. Nucl. Med.* **2007**, *48*, 1313–9.

(10) Wang, H.; Cai, W.; Chen, K.; Li, Z. B.; Kashefi, A.; He, L.; Chen, X. A new PET tracer specific for vascular endothelial growth factor receptor 2. *Eur. J. Nucl. Med. Mol. Imaging* **2007**, *34*, 2001–10.

(11) Collingridge, D. R.; Carroll, V. A.; Glaser, M.; Aboagye, E. O.; Osman, S.; Hutchinson, O. C.; Barthel, H.; Luthra, S. K.; Brady, F.; Bicknell, R.; Price, P.; Harris, A. L. The development of [(124)I]iodinated-VG76e: a novel tracer for imaging vascular endothelial growth factor in vivo using positron emission tomography. *Cancer Res.* **2002**, *62*, 5912–9.

(12) Li, S.; Peck-Radosavljevic, M.; Koller, E.; Koller, F.; Kaserer, K.; Kreil, A.; Kapiotis, S.; Hamwi, A.; Weich, H. A.; Valent, P.; Angelberger, P.; Dudczak, R.; Virgolini, I. Characterization of (123)I-vascular endothelial growth factor-binding sites expressed on human tumour cells: possible implication for tumour scintigraphy. *Int. J. Cancer* **2001**, *91*, 789–96.

(13) Backer, M. V.; Levashova, Z.; Patel, V.; Jehning, B. T.; Claffey, K.; Blankenberg, F. G.; Backer, J. M. Molecular imaging of VEGF receptors in angiogenic vasculature with single-chain VEGF-based probes. *Nat. Med.* **2007**, *13*, 504–9.

(14) Blankenberg, F. G.; Backer, M. V.; Levashova, Z.; Patel, V.; Backer, J. M. In vivo tumor angiogenesis imaging with site-specific labeled (99m)Tc-HYNIC-VEGF. *Eur. J. Nucl. Med. Mol. Imaging* **2006**, *33*, 841–8.

(15) Korpanty, G.; Carbon, J. G.; Grayburn, P. A.; Fleming, J. B.; Brekken, R. A. Monitoring response to anticancer therapy by targeting microbubbles to tumor vasculature. *Clin. Cancer Res.* **2007**, *13*, 323–30.

(16) Willmann, J. K.; Paulmurugan, R.; Chen, K.; Gheysens, O.; Rodriguez-Porcel, M.; Lutz, A. M.; Chen, I. Y.; Chen, X.; Gambhir, S. S. US imaging of tumor angiogenesis with microbubbles targeted to vascular endothelial growth factor receptor type 2 in mice. *Radiology* **2008**, *246*, 508–18.

(17) Backer, M. V.; Patel, V.; Jehning, B. T.; Backer, J. M. Self-assembled "dock and lock" system for linking payloads to targeting proteins. *Bioconjugate Chem.* **2006**, *17*, 912–9.

(18) Lu, E.; Wagner, W. R.; Schellenberger, U.; Abraham, J. A.; Klibanov, A. L.; Woulfe, S. R.; Csikari, M. M.; Fischer, D.; Schreiner, G. F.; Brandenburger, G. H.; Villanueva, F. S. Targeted in vivo labeling of receptors for vascular endothelial growth factor: approach to identification of ischemic tissue. *Circulation* **2003**, *108*, 97–103.

(19) Li, S.; Peck-Radosavljevic, M.; Kienast, O.; Preitfellner, J.; Hamilton, G.; Kurtaran, A.; Pirich, C.; Angelberger, P.; Dudczak, R. Imaging gastrointestinal tumours using vascular endothelial growth factor-165 (VEGF165) receptor scintigraphy. *Ann. Oncol.* **2003**, *14*, 1274–7.

(20) Li, S.; Peck-Radosavljevic, M.; Kienast, O.; Preitfellner, J.; Havlik, E.; Schima, W.; Traub-Weidinger, T.; Graf, S.; Beheshti, M.; Schmid, M.; Angelberger, P.; Dudczak, R. Iodine-123-vascular endothelial growth factor-165 (123I-VEGF165). Biodistribution, safety and radiation dosimetry in patients with pancreatic carcinoma. *Q. J. Nucl. Med. Mol. Imaging* **2004**, *48*, 198–206.

(21) Blankenberg, F. G.; Mandl, S.; Cao, Y. A.; O'Connell-Rodwell, C.; Contag, C.; Mari, C.; Gaynutdinov, T. I.; Vanderheyden, J. L.; Backer, M. V.; Backer, J. M. Tumor imaging using a standardized radiolabeled adapter protein docked to vascular endothelial growth factor. *J. Nucl. Med.* **2004**, *45*, 1373–80.

(22) Choi-Rhee, E.; Schulman, H.; Cronan, J. E. Promiscuous protein biotinylation by Escherichia coli biotin protein ligase. *Protein Sci.* **2004**, *13*, 3043–50.

Scheme 1. Schematic Representation of the Preparation of Site-Specifically Labeled VEGF for Near-Infrared Fluorescence (NIRF) Imaging[a]

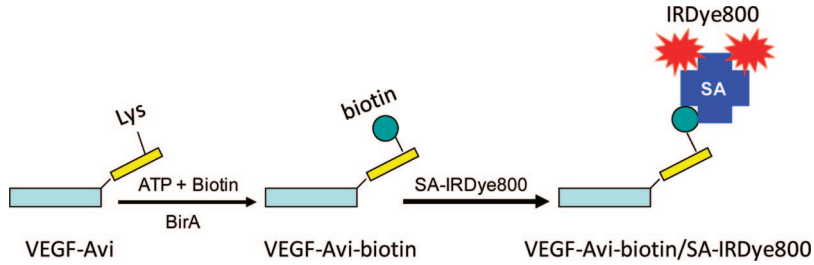

[a] Step 1: Synthesis of Avi-tagged VEGF protein. Step 2: Reaction of VEGF-Avi protein with BirA and biotin to form site-specifically biotinylated $VEGF_{121}$-Avi-biotin (VEGF-Avib). Step 3: Reaction of VEGF-Avi-biotin with streptavidin-IRDye800 (SA800) to form VEGF-Avib/SA800 complex for in vivo NIRF imaging.

Experimental Section

Cell Lines and Animal Model. Porcine aortic endothelial (PAE) cells that express human KDR (PAE/KDR)[10] were cultured in Ham's F-12 medium containing 10% fetal calf serum (FBS) (Invitrogen). The 67NR murine breast cancer cell line (kindly provided by Dr. Fred R. Miller, Karmanos Cancer Institute)[23] was cultured in high-glucose DMEM medium containing 10% FBS. Animal experiments were carried out according to a protocol approved by Stanford University Institutional Animal Care and Use Committee (IACUC). Female athymic nude mice (4−6 weeks old) were obtained from Harlan (Indianapolis, IN). The 67NR tumor model was generated by injection of 5×10^6 67NR cells in 100 μL of PBS into the front left flank of each mouse. The mice were subjected to Maestro optical imaging studies when the tumor volume reached about 100−200 mm^3.

Generation and Characterization of Avi-Tagged Proteins. The fusion gene encoding VEGF-Avi, VEGF-Avi(K/S) or $VEGF_m$-Avi was prepared by DNA recombinant technology. The fusion proteins were expressed in *Escherichia coli* and purified by Ni-NTA affinity chromatography. The detailed procedure is available from the Supporting Information. The binding affinity of various VEGF molecules to PAE/KDR cells was determined by a competitive cell binding experiments using ^{125}I-labeled $VEGF_{165}$ as the radioligand as described before.[10] The best-fit IC_{50} values were calculated by fitting the data by nonlinear regression using GraphPad Prism. Experiments were carried out with triplicate samples.

Biotinylation of Avi-Tagged VEGF Proteins. The site-specific biotinylation of Avi-tagged VEGF proteins was performed using BirA enzyme. The following reaction was set up for BirA mediated biotinylation: a mixture of 1 nmol of purified Avi-tagged proteins in 23 μL of PBS, 3 μL of BioMixA (0.05 M bicine buffer, pH 8.3), 3 μL of BioMixB (10 mM ATP, 10 mM $Mg(OAc)_2$, 5 μM D-biotin) and 1 μL of BirA (1 mg/mL, 5000 units/μg) (GeneCopoeia, Germantown, MD) was incubated at 30 °C for 30 min. We also set up control experiments for VEGF-Avi in which either biotin or BirA was omitted from the reaction. For chemical biotinylation of $VEGF_{121}$, EZ-link NHS-PEG12-Biotin (Pierce, Rockford, IL) and $VEGF_{121}$-Avi protein were mixed at a molar ratio of 3:1. The mixture was incubated at room temperature for 1 h, and biotinylated $VEGF_{121}$ was purified by NAP-10 column (GE healthcare).

Characterization of Biotinylated VEGF-Avi. The biotinylation of Avi-tagged proteins was identified by probing the biotinylated protein with streptavidin conjugated horseradish peroxidase (SA-HRP) using Western blot. The interaction of biotinylated Avi-tagged VEGF (VEG-Avib) with streptavidin was confirmed by comparing the motility of SA-HRP and VEGF-Avib/SA-HRP complex or by ELISA. The detailed experiment protocols are available from Supporting Information.

Cell Staining. To test whether $VEGF_{121}$-Avi-bio/SA-Cy5.5 (VEGF-Avib/SA-Cy) retains its ability to bind to VEGFR2, we performed a staining experiment using PAE and PAE/KDR cells. Streptavidin-Cy5.5 (SA-Cy, 50 nmol in 25 μL of PBS) was incubated with VEGF-Avib (200 nmol in 100 μL of PBS) to form a stable complex of VEGF-Avib/SA-Cy. The PAE cells and PAE/KDR cells were seeded in glass bottom culture dishes (MatTek) the day before staining. After rinsing with PBS buffer twice, VEGF-Avib/SA-Cy or SA-Cy (10 nmol) in serum-free F-12 Hams growth medium (Invitrogen) was added and incubated for 30 min at RT. After rinsing with PBS buffer, the cells were examined under an inverted epifluorescence microscope (Carl Zeiss).

***In Vivo* and *ex Vivo* NIRF Imaging.** The 67NR tumor mice were imaged at multiple time points post injection (p.i.) using the Maestro *in vivo* imaging system (CRI, Woburn, MA; excitation = 735 nm, emission = 780 nm long pass). After the last *in vivo* images were collected at 66 h p.i., the mice were sacrificed; 67NR tumor and major organs were harvested and subjected to *ex vivo* NIRF imaging immediately. The acquisition condition was the same as *in vivo* imaging. The tissues were weighted to normalize NIRF signals.

Immunofluorescence Staining. Forty hours after intravenous injection of VEGF-Avib/SA-Cy or SA-Cy (0.5 nmol

(23) Aslakson, C. J.; Miller, F. R. Selective events in the metastatic process defined by analysis of the sequential dissemination of subpopulations of a mouse mammary tumor. *Cancer Res.* **1992**, *52*, 1399–405.

of Cy5.5 equivalent per mouse), tumors were collected and fixed in 4% paraformaldehyde, then frozen cut into slices of 30 μm. Sections were stained with anti-CD31 (1:100) and anti-VEGFR2 (1:100) antibodies 1 h at RT, then incubated with FITC-conjugated secondary antibody (1:200, Jackson ImmunoResearch Laboratories) for 1 h. The slices were mounted with medium containing DAPI (Vector Laboratories) and examined under a laser scanning confocal microscope (LSM510, Carl Zeiss). We performed confocal experiments for all the slices in parallel with each probe in order to confirm the specificity of antibody labeling, and to be sure that the staining density and intensity remained the same under all circumstances.

Statistical Analysis. Quantitative data were expressed as mean ± SD. Statistical analysis was done using unpaired Student *t* test for comparisons between groups. Statistical significance was established at $p < 0.05$.

Other Methods. Detailed procedures for protein expression, purification and characterization, Western blot, ELISA and sample preparation for peptide mass mapping are described in the Supporting Information.

Results

Site-Specific Biotinylation of VEGF-Avi. After we purified Avi-tagged proteins, we incubated VEGF-Avi (Supplementary Figure 1 in the Supporting Information), $VEGF_m$-Avi or VEGF-Avi(K/S) with BirA and biotin at room temperature for 30 min. Detailed biosynthesis of the Avi-tagged proteins and biotinylation of the fusion protein can be found as Supplementary Methods in the Supporting Information. Both VEGF-Avi and $VEGF_m$-Avi can be successfully biotinylated in the presence of BirA (Figure 1a), whereas VEGF-Avi(K/S) cannot be biotinylated by BirA. Because VEGF-Avi(K/S) has the same amino acid sequence as VEGF-Avi except for one lysine to serine mutation within the Avi tag, we can conclude that BirA mediated biotinylation happens only on this particular lysine, but not on any other 4 lysines on the $VEGF_{121}$ protein.

To test whether site-specifically biotinylated VEGF-Avi (VEGF-Avib) retains its ability to complex with streptavidin (SA), we performed the following two experiments. First, we mixed VEGF-Avib with streptavidin-horseradish peroxidase conjugates (SA-HRP) for 5 min, then the reaction mixture was mixed with SDS-PAGE sample buffer and loaded onto 4−12% SDS−PAGE gel under reducing conditions without heating for separation. The protein bands were visualized by Coomassie blue staining (Supplementary Figure 2 in the Supporting Information). The molecular weight difference between VEGF-Avib/SA-HRP and SA-HRP suggests a 1:1 complex between VEGF-Avib and SA-HRP. In addition, we performed ELISA using different amount of immobilized VEGF-Avib and same amount of streptavidin-Cy5.5 (SA-Cy, 10 μg/100 μL), the SA-Cy fluorescence intensity increased proportionally to the logarithm of the coated VEGF-Avib concentration (Figure 1b) ($R^2 = 0.73$). These results confirm that site-specifically biotinylated VEGF-Avi protein (VEGF-Avib) is able to form stable complexes with streptavidin conjugates.

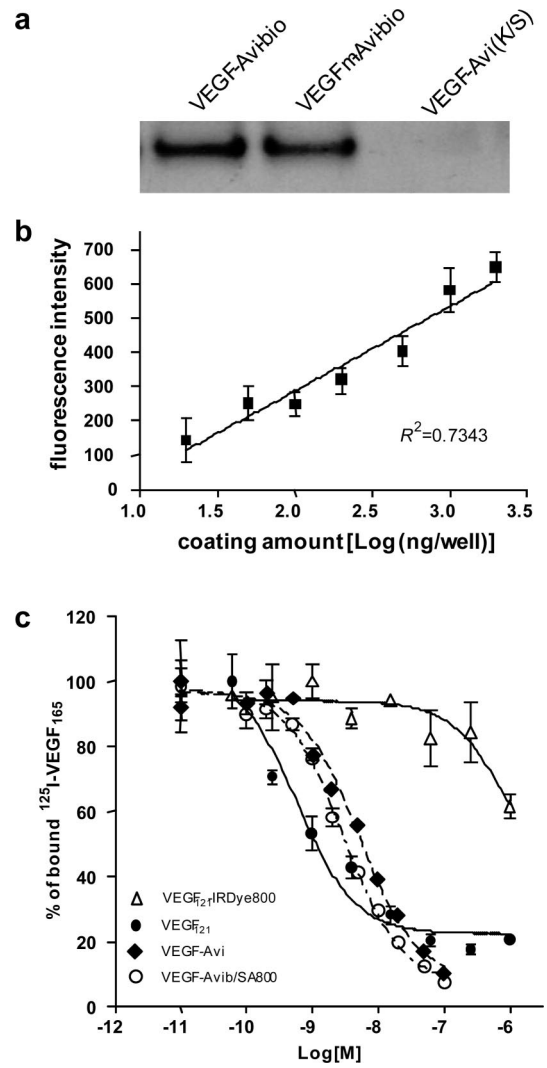

Figure 1. Characterization of VEGF-Avi-biotin/streptavidin (VEGF-Avib/SA) complexes. (a) VEGF-Avi and $VEGF_m$-Avi, but not VEGF-Avi(K/S), can be biotinylated by incubation with BirA and biotin at room temperature for 30 min as analyzed by Western blotting. (b) ELISA confirms that VEGF-Avib retains its ability to form complex with SA-Cy. (c) Receptor binding assay using ^{125}I-$VEGF_{165}$ as radioligand shows that VEGF-Avi and VEGF-Avib/SA800 but not chemically modified VEGF-Avi-IRDye800 (VEGF-Avi/800) retained high affinity for VEGFR-2 expressed on PAE/KDR cells.

After we have assessed that VEGF-Avi protein can be successfully biotinylated in a site-specific manner, and the resulting VEGF-Avib can form a stable complex with streptavidin, we then set out to test whether VEGF-Avib/SA800 complex retains its ability to bind to VEGFRs. To address this, we first performed a cell binding assay using PAE/KDR cells as previously described.[10] The VEGFR-2 binding affinity values of the wild-type $VEGF_{121}$, VEGF-Avi, and VEGF-Avib/SA800 were 0.72 ± 0.41, 5.18 ± 1.29, and 3.09 ± 1.15 nM, respectively. Compared with wild-type $VEGF_{121}$, the binding affinity

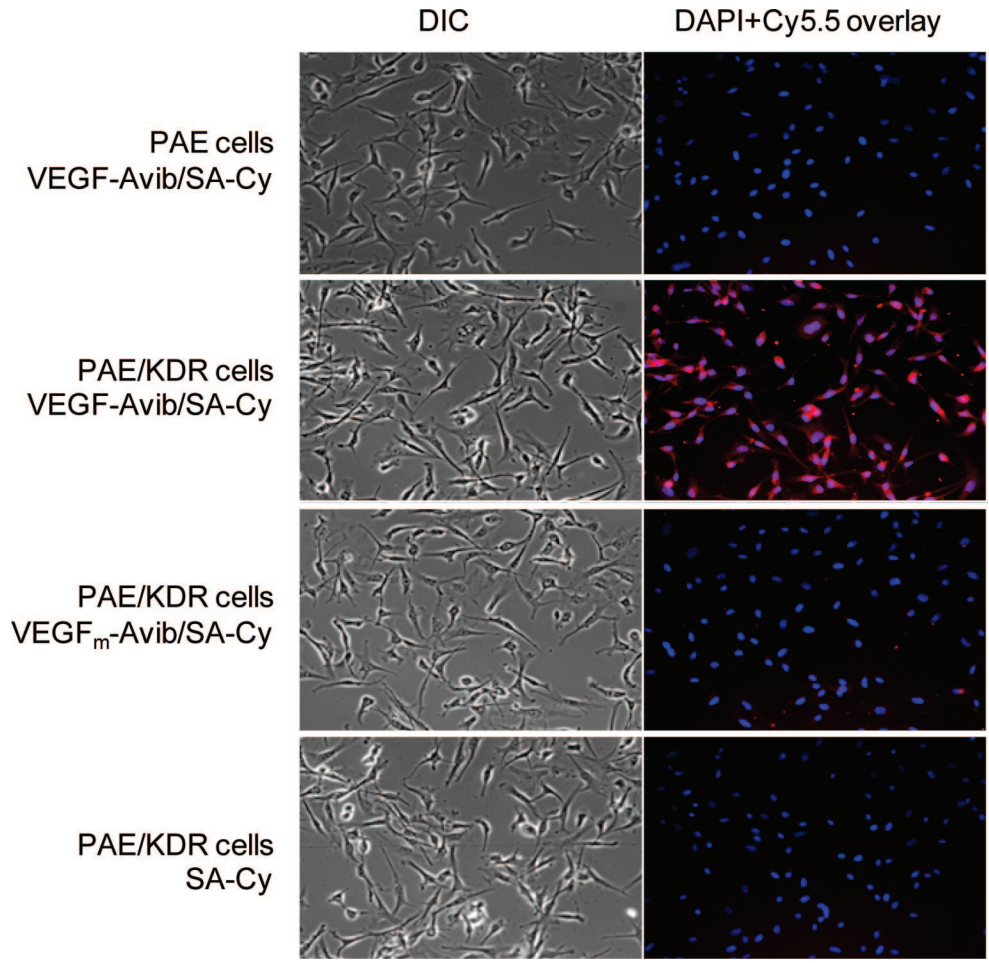

Figure 2. Cell staining of Cy5.5 conjugates. Differential interference contrast (DIC) and epifluorescence images of PAE cells with VEGF-Avib/SA-Cy and PAE/KDR cells with VEGF-Avib/SA-Cy, VEGF$_m$-Avib/SA-Cy and SA-Cy. Positive cell staining is only possible for VEGF-Avib/SA-Cy incubation with PAE/KDR cells, confirming VEGFR specificity of this biotin/streptavidin complex.

of VEGF-Avi and VEGF-Avib/SA800 to VEGFR-2 was only slightly decreased. In contrast, the binding affinity of chemically modified VEGF-Avi-IRDye800 (VEGF-Avi/800), which was formed by chemical conjugation of IRDye800-NHS ester with VEGF$_{121}$, was as low as 3.03 $\pm$ 0.79 μM, which is decreased by 3 orders of magnitude as compared with VEGF$_{121}$ (Figure 1c). Second, we stained PAE and PAE/KDR cells with VEGF-Avib/SA-Cy, VEGF$_m$-Avib/SA-Cy and SA-Cy. We used Cy5.5 instead of IRDye800 conjugates for cell staining because the emission wavelength of IRDye800 (806 nm) is beyond the optimal detection capacity of our inverted epifluorescence microscope. Nevertheless, our staining results showed that VEGF-Avib/SA-Cy binds well to PAE/KDR cells but not to PAE cells. VEGF$_m$-Avib/SA-Cy showed very weak PAE/KDR cell staining due to the low binding affinity of VEGF$_m$ to both VEGFR-1 and VEGFR-2.[24] As a control, SA-Cy showed virtually no binding to PAE/KDR cells (Figure 2).

In Vivo **Near-Infrared Fluorescence Imaging.** After verifying that VEGF-Avib/SA800 complex is fully functional with regard to its receptor binding affinity and specificity, we proceeded to test the complex in living subjects. Nude mice bearing subcutaneous 67NR tumors (3 weeks postinoculation of 5×10^6 cells on the front flank when the tumor size reached 6−10 mm in diameter) were divided into 4 groups (n = 4/group), and each group of animals received intravenous injection of VEGF-Avib/SA800, VEGF$_m$-Avib/SA800, VEGF-Avi/800, or SA800 (0.5 nmol of IRDye800 equivalent per mouse). The mice were then imaged at multiple time points postinjection (p.i.) using the Maestro *in vivo* imaging system. After image acquisition, spectral unmixing yielded the pseudocolor images of the pure spectrum of IRDye800. Representative sagittal images are shown in Figure 3a. The same region of interest (ROI) was drawn for each tumor over time, and the total signals were

(24) Willmann, J. K.; Chen, K.; Wang, H.; Paulmurugan, R.; Rollins, M.; Cai, W.; Wang, D. S.; Chen, I. Y.; Gheysens, O.; Rodriguez-Porcel, M.; Chen, X.; Gambhir, S. S. Monitoring of the biological response to murine hindlimb ischemia with 64Cu-labeled vascular endothelial growth factor-121 positron emission tomography. *Circulation* **2008**, *117*, 915–22.

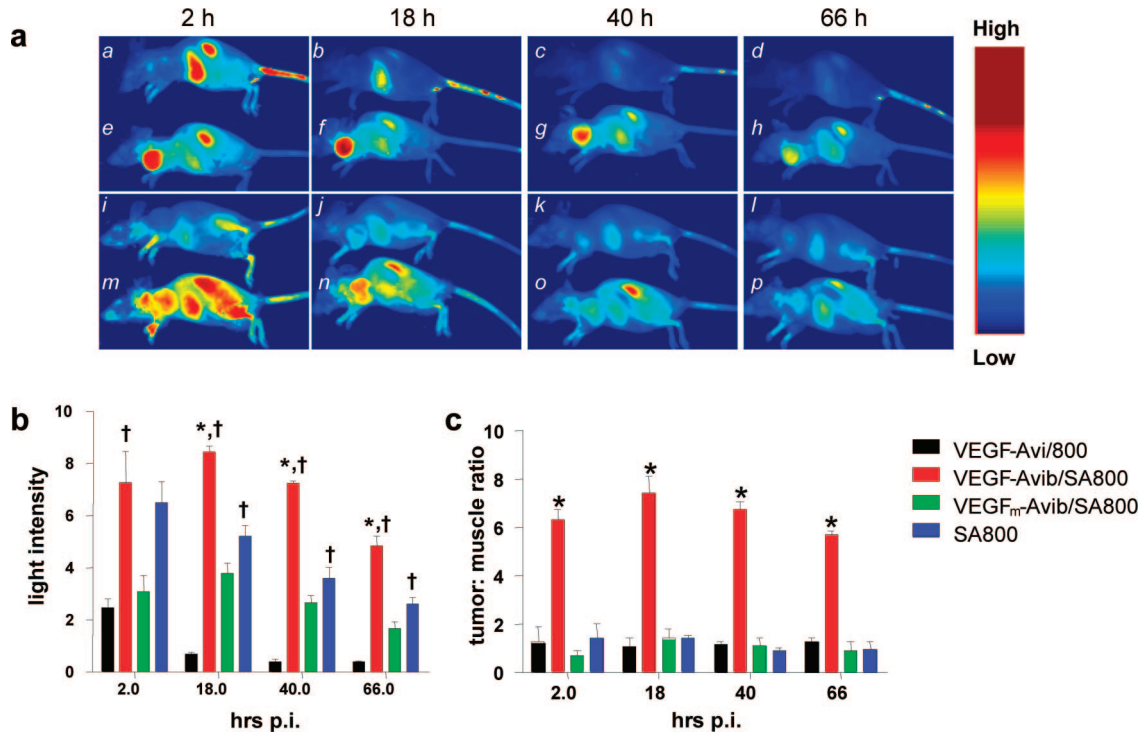

Figure 3. *In vivo* imaging of 67NR tumors with IRDye800 conjugates. (a) Representative sagittal images at 2, 18, 40 and 66 h after intravenous injection of chemically modified $VEGF_{121}$-Avi-IRDye800 (VEGF-Avi/800) (*a*–*d*), $VEGF_{121}$-Avi-biotin/streptavidin-IRDye800 (VEGF-Avib/SA800) (*e*–*h*), $VEGF_{mutant}$-Avi-biotin/streptavidin-IRDye800 ($VEGF_m$-Avib/SA800) (*i*–*l*), and streptavidin-IRDye800 (SA800) (*m*–*p*). All images were acquired and processed under the same conditions. Total fluorescence signals normalized by exposure time and ROI area (total signal/ms·mm^2). (b) Tumor light intensity and (c) tumor to muscle light intensity ratio at multiple time points after i.v. injection of appropriate probes. Columns, means; bars, SE. *, VEGF-Avib/SA800 compared with SA800, statistically significant ($p < 0.05$). †, VEGF-Avib/SA800 compared with VEGF-Avi/800, statistically significant ($p < 0.05$). ($n = 4$/group.)

normalized by the exposure time and tumor size [total signal/ms·mm^2]. VEGF-Avi/800 showed no tumor accumulation (Figure 3a, *a*–*d*) at all time points examined and was cleared rapidly via the renal route due to its relatively small molecular size. VEGF-Avib/SA800 had rapid and high tumor uptake and contrast (Figure 3a, *e*–*h*). $VEGF_m$-Avib/SA800 showed minimal tumor uptake as compared with VEGF-Avib/SA800 because of the substantially lower binding affinity of $VEGF_m$ moiety to both VEGFR-1 and VEGFR-2 (Figure 3a, *i*–*l*). SA800 showed longer circulation and thus higher background signal than VEGF-Avib/SA800, which is partially attributed to the wide distribution of endogenous biotin in small amounts in the blood (~10 nM) and various tissues.[25] The presence of early tumor contrast and then clearance from the tumor area observed from SA800 injection is likely due to the passive targeting of high molecular weight molecules such as SA800 via the enhanced permeability and retention (EPR) effect (Figure 3a, *m*–*p*). The tumor fluorescence signals quantification derived from the 2-dimensional images were illustrated in Figure 3b. VEGF-Avib/SA800 had significantly higher tumor signal intensity than VEGF-Avi/800 ($p = 0.0179$, $p < 0.0001$, $p = 0.0005$, and $p = 0.001$ at 2 h, 18 h, 40 and 66 h p.i., respectively) and $VEGF_m$-Avib/SA800 ($p = 0.0359$, $p = 0.0005$, $p = 0.0038$, and $p = 0.0081$ at 2 h, 18 h, 40 and 66 h p.i., respectively) at all time points. There is little difference between VEGF-Avib/SA800 and SA800 at 2 h p.i. ($p = 0.6247$) in terms of tumor signal intensity, but at late time points it is clear that tumor signal from VEGF-Avib/SA800 is significantly higher than SA800 ($p = 0.0022$, $p = 0.0038$, and $p = 0.0001$ at 18 h, 40 and 66 h, p.i., respectively). It is also of note that the tumor-to-background ratio coming from VEGF-Avib/SA800 is significantly higher than VEGF-Avi/800 ($p = 0.0028$, $p = 0.0014$, $p < 0.0001$, and $p < 0.0001$ at 2 h, 18 h, 40 and 66 h, p.i., respectively), $VEGF_m$-Avib/SA800 ($p = 0.003$, $p = 0.0018$, $p = 0.0002$, and $p = 0.003$ at 2 h, 18 h, 40 and 66 h p.i., respectively), and SA800 ($p = 0.0027$, $p = 0.0012$, $p < 0.0001$, and $p = 0.0002$ at 2 h, 18 h, 40 and 66 h p.i., respectively) at all time points (Figure 3c).

***In Situ* Validation of *in Vivo* Imaging Results.** *Ex vivo* NIRF images of the organs extracted from 66 h after tracer injection are shown in Supplementary Figure 3 in the Supporting Information. The average fluorescence intensity (total signal/ms·mm^2) of all 4 tracers in the tumor and major

(25) Mock, D. M.; DuBois, D. B. A sequential, solid-phase assay for biotin in physiologic fluids that correlates with expected biotin status. *Anal. Biochem.* **1986**, *153*, 272–8.

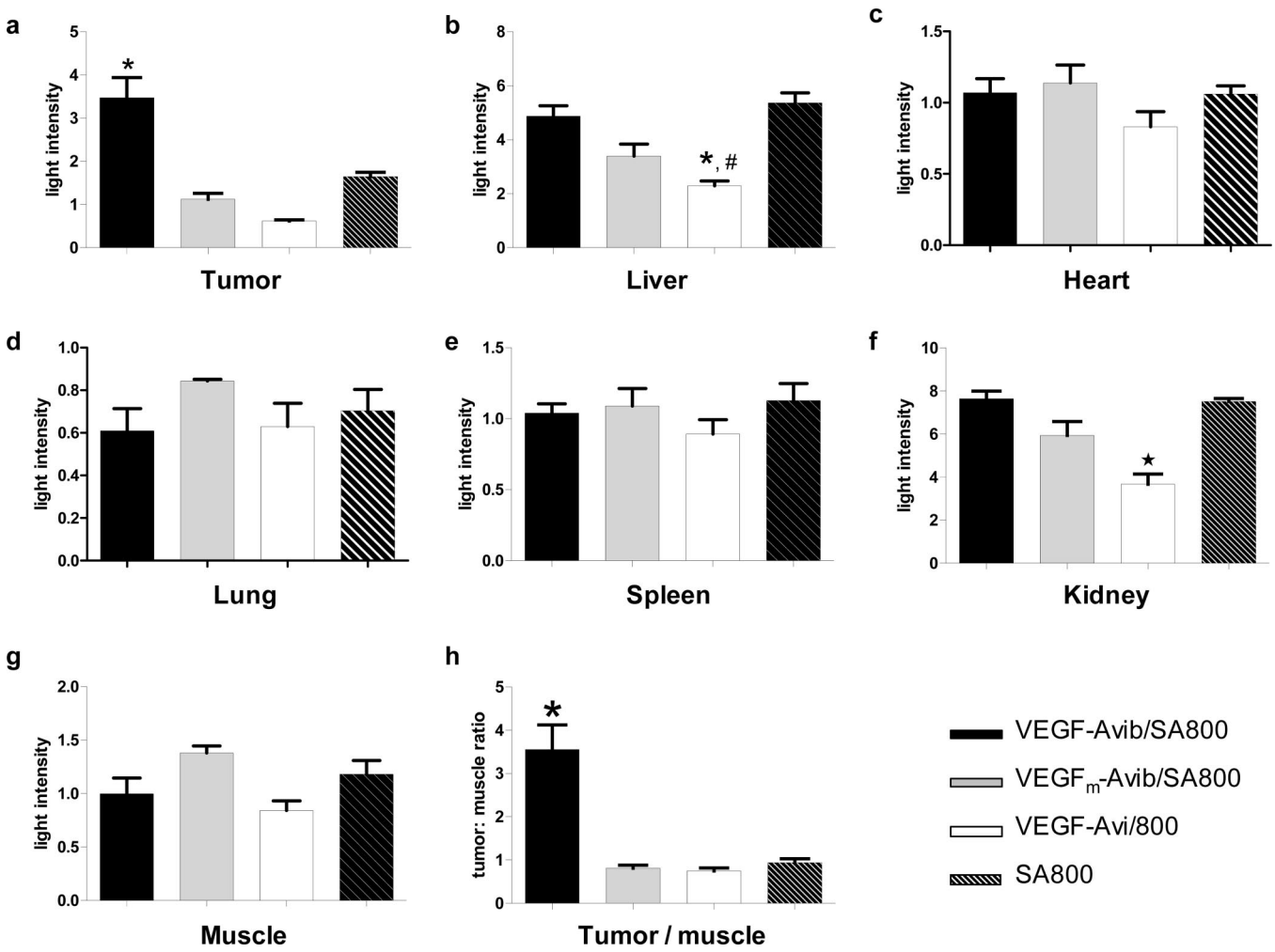

Figure 4. Probe biodistribution at 66 h p.i. by *ex vivo* NIRF imaging. The light intensity of VEGF-Avib/SA800 (black column), VEGF$_m$-Avib/SA800 (gray column), VEGF-Avi/800 (hollow column) and SA800 (striped column) at 66 h p.i. in tumor (a), liver (b), heart (c), lung (d), spleen (e), kidneys (f), muscle (g) and tumor to muscle signal ratio (h) were compared. Columns, means; bars, SE. $*$ in a, VEGF-Avib/SA800 compared with VEGF-Avi/800, statistically significant ($p < 0.05$). $*$ in b, VEGF-Avi/800 compared with VEGF-Avib/SA800, statistically significant ($p < 0.05$). # in b, VEGF-Avi/800 compared with SA800, statistically significant ($p < 0.05$). ★ in f, VEGF-Avi/800 compared with VEGF-Avib/SA800, statistically significant ($p < 0.05$). $*$ in h, VEGF-Avib/SA800 compared with SA800, statistically significant ($p < 0.05$).

organs is shown in Figure 4, *a*−*g*. In all the major organs we collected, liver showed high and comparable fluorescence intensity from mice receiving VEGF-Avib/SA800 (Supplementary Figure 3b in the Supporting Information), VEGF$_m$-Avib/SA800 (Supplementary Figure 3c in the Supporting Information) and SA800 (Supplementary Figure 3d in the Supporting Information), while the liver fluorescence intensity from mice receiving VEGF-Avi/800 (Supplementary Figure 3a in the Supporting Information) was significantly lower than that from VEGF-Avib/SA800 ($p = 0.0035$) and SA800 ($p = 0.0017$) groups (Figure 4b). Similar results were also observed in the kidneys: kidney fluorescence intensity from mice receiving VEGF-Avi/800 was significantly lower than that from VEGF-Avib/SA800 ($p = 0.0025$), VEGF$_m$-Avib/SA800 ($p = 0.0459$) and SA800 ($p = 0.0014$) groups, respectively (Figure 4f). The lower liver and kidney accumulation of VEGF-Avi/800 is presumably due to the fast clearance of the low molecular weight protein conjugate. The average fluorescence signal of VEGF-Avib/SA800 from tumor tissue was significantly higher than that of the other three tracers at 66 h p.i. ($p = 0.0085$, $p = 0.0037$ and $p = 0.0187$ vs VEGF$_m$-Avib/SA800, VEGF-Avi/800 and SA800, respectively), which corroborates with the data obtained from the *in vivo* imaging studies. Considering the high fluorescence signal background in the mice receiving SA800 injection due to the unfavorable pharmacokinetics of SA, the tumor:muscle ratio of the VEGF-Avib/SA800 was significantly much higher than other three tracers ($p = 0.0084$, $p = 0.0078$ and $p = 0.0225$ vs VEGF$_m$-Avib/SA800, VEGF-Avi/800 and SA800, respectively, Figure 4h), which further demonstrates the specific binding of VEGF-Avib/SA800 to VEGFRs in the tumor. There is no significant difference of the accumulation of these four tracers in other organs, such as heart, lung, spleen and muscles (Figure 4c,d,e,g).

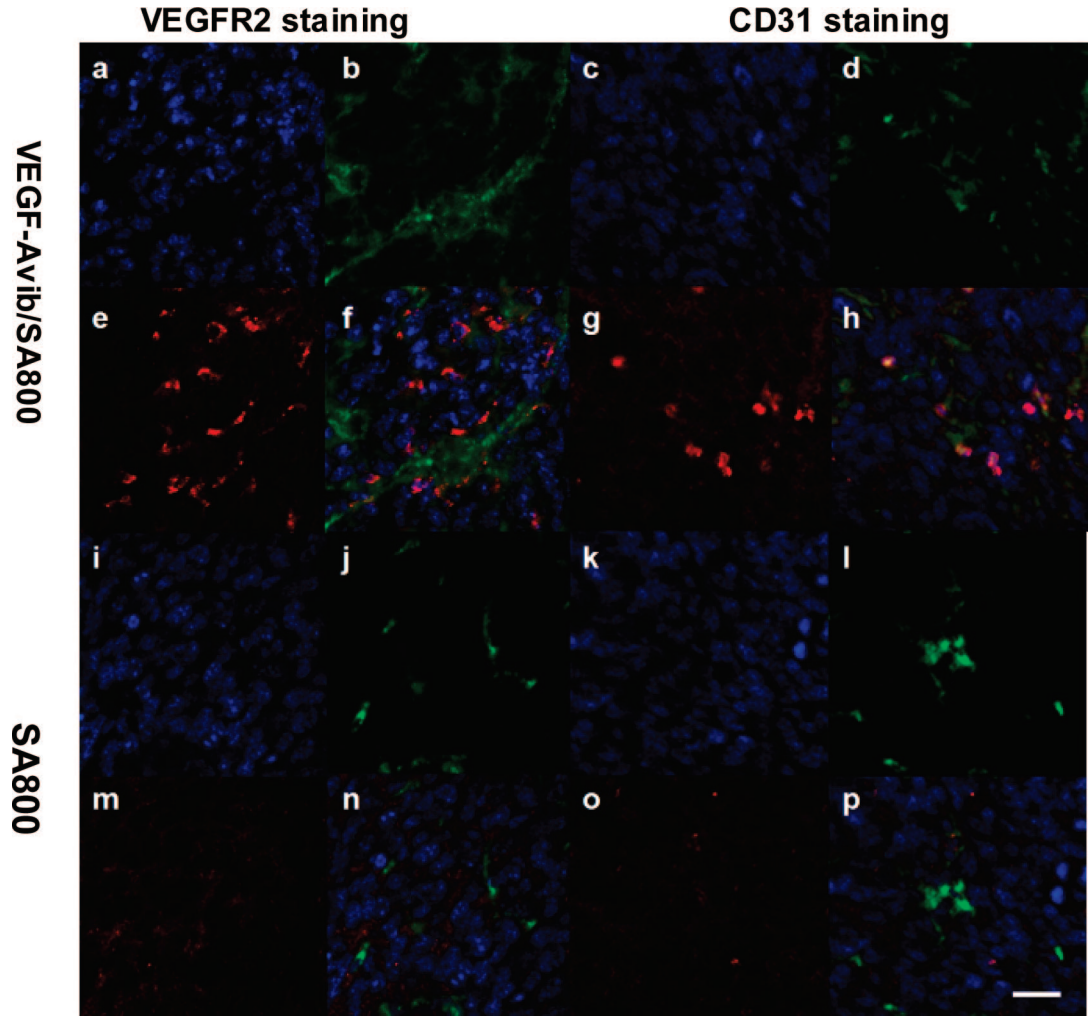

Figure 5. Regional localization of VEGF-Avib/SA-Cy and SA-Cy within tumors. Immunofluorescence images of frozen tumor sections prepared 40 h after VEGF-Avib/SA-Cy (a−h) and SA-Cy (i−p) injections. VEGFR2 and CD31 signals were coded green, and Cy5.5 signals were coded red. DAPI signals were coded blue.

To further characterize the cellular distribution of VEGF-Avib/SA800 and SA800, we injected the animals with fluorescent dye conjugates, sacrificed the mice at 40 h p.i., and analyzed the tumor specimens for VEGFR2 and CD31 (tumor vasculature) by immunofluorescence staining (Figure 5). Due to the fluorescence microscope limitation, we used Cy5.5 conjugates (SA-Cy) instead of IRDye800 conjugates (SA800). We examined VEGFR2 positive cells and CD31 positive tumor vessels in order to elucidate the VEGF-Avib/SA-Cy binding pattern. It is of note that the binding of VEGF-Avib/SA-Cy on the luminal endothelial cells happened mainly in a multiple, discrete and patched form (Figure 5, *e*−*h*) colocalized with tumor vessels. Fluorescence was also visible on some tumor cells. In sharp contrast, SA-Cy showed a diffused distribution pattern within the tumor, mainly localized in the tumor interstitial space without overlay with tumor vasculature and VEGFR2 positive cells (Figure 5, *m*−*p*).

Discussion

Imaging tumor angiogenesis requires optimization and characterization of the appropriate imaging probes. In this study, we report on the development and validation of site-specifically modified $VEGF_{121}$ protein for noninvasive NIRF imaging of VEGFR expression in murine breast cancer xenografted mice. We designed an Avi-tagged VEGF protein for site-specific biotinylation by BirA enzyme. The biotinylated VEGF-Avi (VEGF-Avi-bio) was mixed with SA-dye, and the resulting VEGF-Avib/SA-dye conjugate was able to image VEGFR expression *in vivo* in a highly efficient and specific manner.

$VEGF_{121}$ has been successfully used for noninvasive imaging VEGFR expression, however, the development of VEGF-based imaging probes for clinical translation is a significant challenge that requires uniform preparation of functionally active conjugates. A 15 amino acid N-terminal fragment of human ribonuclease I with the R4C substitution (Cys-tag) has been incorporated into VEGF protein or single-chain (sc) VEGF protein for site-specific labeling with contrast agents for NIRF, SPECT[14] and PET.[13,17] Cys-tag itself can also form a stable chelate with ^{99m}Tc using Sn(II)-tricine as an exchange reagent.[26] However, the Cys-tagged protein was refolded in the red-ox buffer containing glutathione, the thiol group in Cys-tag was "protected" in mixed

disulfide bond with glutathione,[13] and therefore, it needs to be "deprotected" by incubation with equimolar amounts of DTT for the following site-specific modification or direct chelating with ^{99m}Tc, which is technically very challenging. In addition, different proteins contain different amounts of cysteine, and the cysteine usually plays an important role in maintaining protein's function; addition of extra cysteines will sometimes compromise the protein activity. As a result, we tried to seek alternative strategies for site-specific modification of $VEGF_{121}$ protein as a beneficiary complement to Cys-containing tag. Avi tag, a 14 aa peptide, contains a central lysine residue that can be biotinylated at the epsilon amine group by the bacteria BirA biotin ligase. Coexpression of a tagged protein and the BirA gene in cells results in a highly specific, quantitative biotinylation of the tagged protein.[27] To take the advantage of highly sequence specific biotinylation Avi-tagged protein by BirA and the strongest noncovalent biological interaction between biotin and streptavidin, we designed $VEGF_{121}$-Avi fusion protein. The $VEGF_{121}$-Avi protein binds to PAE/KDR cells with high affinity and can be quantitatively biotinylated by BirA in a site-specific manner, and the biotinylated VEGF-Avi is able to form a stable complex with SA protein, SA-HRP, or SA-dye conjugates. The VEGF-Avib/SA800 complex retained the binding ability of VEGF moiety to PAE/KDR cells. On the other hand, chemical conjugation of near-infrared dye IRDye800 to $VEGF_{121}$ led to almost complete inactivation of $VEGF_{121}$ (Figure 1c). Injection of VEGF-Avi/800 into 67NR-tumor bearing mice showed fast clearance from circulation and no tumor accumulation over time. In contrast, site-specific modified VEGF-Avib/SA800 showed rapid and high tumor accumulation and sustained tumor to background contrast (Figure 3a, *e*−*h*).

$VEGF_{121}$ can also be biotinylated by the NHS-esters or sulfo-NHS-esters of biotin under slightly basic condition. Unlike chemical modification with the bulky fluorescent dyes such as Cy5.5 and IRDye800, low level of random biotinylation (less than 1:1 ratio) seems to have little effect on the receptor binding affinity of the biotin conjugate. The main concern of chemical conjugation of $VEGF_{121}$ with NHS-esters or sulfo-NHS-esters of biotin is that $VEGF_{121}$ has one N-terminal α-amine and 4 lysine epsilon-amines, and there is no control over which amine group will be modified and which modification will retain the receptor avidity. Apart from potent ability to image VEGFRs expression *in vivo*, a site-specifically modified VEGF probe offers additional advantages: (1) the modification happens only on the designed lysine residue at the Avi-tag, leaving all the other 4 lysine residues in $VEGF_{121}$ protein unaffected; (2) using standardized procedures for BirA mediated biotinylation reaction, there will be virtually no variation of biotinylated VEGF-Avi prepared from different batches.

Despite the fact that $VEGF_{121}$ is a strong binder of VEGFRs *in vitro*, the tumor uptake of VEGF-Avib/SA800 *in vivo* may be caused by specific binding of the conjugate with VEGFRs expressed on the tumor, by nonspecific adsorption of the VEGF protein, by the binding of SA-dye conjugates to endogenous biotin, and by EPR effect. To better understand the *in vivo* behavior of VEGF-Avib/SA800 we performed several control experiments. First, an Avi-tagged VEGF mutant was employed to couple with SA-dye. $VEGF_m$-Avib/SA-dye has nearly equivalent size and surface chemistry to VEGF-Avib/SA-dye, yet lacks VEGFR affinity. As a result, $VEGF_m$-Avib/SA-dye had little binding to VEGFR2 positive PAE/KDR cells in culture (Figure 2) and low accumulation in the tumor area (Figure 3a, *i*−*l*; Figure 4a, *c*). ROI analysis of the tumor signals *in vivo* and *ex vivo* further confirms the significant difference between $VEGF_m$-Avib/SA-dye and VEGF-Avib/SA-dye (Figure 3b; Figure 4b). The absence of $VEGF_m$-Avib/SA-dye signal in the tumor excludes the possibility of passive tumor targeting of VEGF-Avib/SA-dye caused by EPR effect in our tumor model. Second, SA-dye conjugate was compared with VEGF-Avib/SA-dye. SA-dye showed no binding to PAE/KDR cells (Figure 2) *in vitro*, however, it did show some extent of tumor uptake at early time points in *in vivo* NIRF imaging (Figure 3a, *m*,*n*), but decreased dramatically after 40 h p.i. (Figure 3a, *o*,*p*; Figure 4). It has been reported that ^{125}I-streptavidin has slow blood clearance and high organ retention.[28] In our study, SA-dye showed similar behavior as ^{125}I-SA with high renal uptake and slow clearance from the circulation. Nevertheless, the tumor fluorescence intensity from VEGF-Avib/SA-dye was significantly higher than that from SA-dye after 40 h p.i. Third, *ex vivo* immunohistochemistry showed diffusive localization of SA-dye in the tumor interstitial space rather than on the endothelial or tumor cell surface while VEGF-Avib/SA-dye are mostly localized on VEGFR-2 positive cells (Figure 5). Taken together, the high tumor uptake of VEGF-Avib/SA-dye at late time points is mediated by VEGF moiety instead of nonspecific binding of SA-dye and passive tumor targeting.

The observation that $VEGF_{121}$-Avi fusion protein can be biotinylated by BirA enzyme and further conjugated with streptavidin-dye for near-infrared fluorescence imaging of tumor VEGFR expression highlights the crucial importance

(26) Levashova, Z.; Backer, M.; Backer, J. M.; Blankenberg, F. G. Direct site-specific labeling of the Cys-tag moiety in scVEGF with technetium 99m. *Bioconjugate Chem.* **2008**, *19*, 1049–54.

(27) Beckett, D.; Kovaleva, E.; Schatz, P. J. A minimal peptide substrate in biotin holoenzyme synthetase-catalyzed biotinylation. *Protein Sci.* **1999**, *8*, 921–9.

(28) Schechter, B.; Silberman, R.; Arnon, R.; Wilchek, M. Tissue distribution of avidin and streptavidin injected to mice. Effect of avidin carbohydrate, streptavidin truncation and exogenous biotin. *Eur. J. Biochem.* **1990**, *189*, 327–31.

(29) Driegen, S.; Ferreira, R.; van Zon, A.; Strouboulis, J.; Jaegle, M.; Grosveld, F.; Philipsen, S.; Meijer, D. A generic tool for biotinylation of tagged proteins in transgenic mice. *Transgenic Res.* **2005**, *14*, 477–82.

(30) Rodriguez, P.; Braun, H.; Kolodziej, K. E.; de Boer, E.; Campbell, J.; Bonte, E.; Grosveld, F.; Philipsen, S.; Strouboulis, J. Isolation of transcription factor complexes by in vivo biotinylation tagging and direct binding to streptavidin beads. *Methods Mol. Biol.* **2006**, *338*, 305–23.

of site-specific modification of $VEGF_{121}$ protein to retain its receptor binding affinity and specificity *in vitro* and *in vivo*. Biotinylation via Avi-tag has been documented and described elsewhere for different applications[29−31] and is manifested here as a robust method to develop protein-based molecular imaging probes in general. Our exploration of optical imaging probes based on Avi-tag strategy may be extended to other avidin, streptavidin, and neutravidin coupled nanoparticles and radionuclides for multimodality imaging studies and eventual clinical translation.

Abbreviations Used

VEGF-Avib, BirA biotinylated $VEGF_{121}$-Avi; SA800, streptavidin-IRDye800; SA-Cy, steptavidin-Cy5.5; SA-HRP, streptavidin-horseradish peroxidase; VEGF-Avib/SA800, $VEGF_{121}$-Avi-bio/SA-IRDye800; $VEGF_m$-Avib, BirA biotinylated $VEGF_{mutant}$-Avi; $VEGF_m$-Avib/SA800, $VEGF_m$-Avi-bio/SA-IRDye800; VEGF-Avib/SA-Cy, $VEGF_{121}$-Avi-bio/SA-Cy5.5; VEGF-Avi/800, chemically labeled VEGF-Avi-IRDye800.

Acknowledgment. We thank Zhaofei Liu for determining the binding affinity of VEGF-Avib/SA800 using cell binding assay; we thank Jinhua Wang for help with confocal microscope. This work was supported in part by National Institutes of Health Grants P50 CA114747 and U54 CA119367 to X.C.

Supporting Information Available: Additional information as noted in the text. This material is available free of charge via the Internet at http://pubs.acs.org.

MP800185H

(31) Smith, P. A.; Tripp, B. C.; DiBlasio-Smith, E. A.; Lu, Z.; LaVallie, E. R.; McCoy, J. M. A plasmid expression system for quantitative in vivo biotinylation of thioredoxin fusion proteins in Escherichia coli. *Nucleic Acids Res.* **1998**, *26*, 1414–20.